Satellite Orbit Transfer and Formation Reconfiguration via an Attitude Control Analogy

Prasenjit Sengupta* **and Srinivas R. Vadali†**

Texas A&M University, College Station, TX 77843-3141

A control law applicable for orbit transfer as well as formation reconfiguration has been developed via a Lyapunov function similar to that used for spacecraft attitude control. It utilizes feedback of kinematic and kinetic error states between the current and desired orbital frames, that are parameterized by Euler parameters, orbit radius and its time derivative, and orbital angular velocities. The efficacy of the control law is demonstrated with examples, including orbit transfers and formation reconfiguration, both with low-eccentricity and high-eccentricity reference orbits, in the presence of J_2 perturbations. Further simplifications in the control law are introduced and it is shown that stability is not affected. A methodology is proposed to reduce control requirement by appropriate gain selection and control initiation at predefined locations. The equivalent impulse requirements obtained for the examples compare very favorably with analytically and numerically optimized figures presented in other published works.

Introduction

The problem of orbital transfers of satellites by the use of continuous, low-thrust control has been studied in great detail. Recent advances in the field of electric propulsion have made low-thrust propulsion an operational reality. Formation flying of spacecraft is also a relatively new area of research wherein control of relative motion is a key element. Control of relative motion requires controlling each satellite's orbit precisely, with high regard for inter-satellite distances, collision hazards, and other

*Graduate Student, Department of Aerospace Engineering, Texas A&M University, College Station, TX 77843-3141, prasenjit@tamu.edu, Student Member, AIAA.

†Stewart & Stevenson-I Professor, Department of Aerospace Engineering, Texas A&M University, College Station, TX 77843-3141, svadali@aero.tamu.edu, Associate Fellow, AIAA.

operational constraints.

The primary purpose of this paper is to develop a Lyapunov-based control law that has a large range of applicability, free from the influence of singularities that arise from the more common descriptions of a satellite's orbit, such as orbital elements. Previous studies in the literature have addressed the problem of continuous-thrust orbit transfer using Lyapunov function-based feedback controllers. Ilgen[1] uses orbital element feedback for orbital transfers, using the classical as well as equinoctial elements. Ilgen's quadratic Lyapunov function is based on only five of the orbital elements. Gurfil[2] uses classical orbital element feedback for orbital transfer and explores nonlinear controllability issues of the problem, and is able to prove by using Gauss variational equations that a spacecraft's orbital elements can be controlled by continuous control, except when the desired orbit is parabolic. Chang et al.[3] approach the problem of orbital transfer by feeding back the angular momentum and eccentricity vectors. References 1–3 provide excellent bases for the development of Lyapunov function-based controllers for formation reconfiguration using orbital elements. Schaub and Alfriend[4] use the local Cartesian coordinates of the Chief/leader satellite and the differential orbital elements between the Deputy/follower satellite and the Chief as feedback. Schaub et al.[5] present two control laws, one in terms of mean elements, and another in terms of inertial coordinates, for formation control, with the added simplification of using mean elements in the presence of J_2 perturbations arising due to a non-spherical Earth model. This reference also proposes a periodic gain-selection procedure, so that individual orbit element errors are corrected at proper locations along the orbit. Naasz[6] uses classical, as well as, equinoctial orbital element feedback for formation control. While the mean anomaly at epoch can be controlled directly, the mean anomaly at the desired time is tracked by specifying a new desired semimajor axis, which asymptotically approaches the original desired semimajor axis. Wang and Hadaegh[7] explore optimal strategies for formation control in rectilinear motion.

Junkins and Turner[8] develop an analogy between orbital motion and rigid body dynamics. In their work, orbital dynamics is characterized by a set of Euler parameters

for describing the kinematics and three angular velocities of the orbit frame with respect to the inertial frame. Kechichian[9] derives relative motion equations based upon a similar model, which account for J_2 and drag perturbations. There are many advantages to such an approach. First, unlike the inertial coordinate description, the kinematic approach offers scope for physical insight into the problem, as will be shown in the model and control law description. Second, unlike control laws that use classical orbital elements, singularities arising due to zero-eccentricity or zero-inclination are very easily avoided if Euler parameters (EPs) are used instead of the 3-1-3 Euler angles, viz., right ascension Ω, inclination i, argument of perigee ω, and true (resp. mean or eccentric) anomaly ν (resp. M or E). Thus it is possible to transfer from or to an equatorial, circular orbit without encountering singularities in the control law. This comes at the added cost of an extra state (four Euler parameters instead of three Euler angles), but EPs also provide a very convenient linear formulation for relative orientations, which is exploited in the derivation of the control law for orbital transfers. Hence, the kinematic approach has the advantages of both the inertial coordinate as well as orbital element approaches. Finally, since satellite ranging provides spacecraft range, range rate, elevation and azimuth, it is convenient to use these quantities directly in the control law.

A set of benchmark problems for spacecraft formation flying missions has been proposed by Carpenter et al.,[10] that include reference low Earth orbit (LEO) and highly elliptical orbit (HEO) missions. The LEO mission benchmark has a near-circular, sun-synchronous reference orbit and the formation is required to be in a 500m projected circular relative orbit. The Magnetosphere Multiscale Mission (MMS)[11] is an example of a HEO formation flight mission, where the apogee and perigee are of the order of 12-30R_e and 1.2R_e, respectively (with R_e denoting the radius of the Earth), yielding eccentricities of the order of 0.8 and higher. The requirement of formation reconfiguration may arise when, for example, one of the Deputies fails, or a change is required in their relative positions with respect to the Chief.

Boundary conditions for establishing formations in low-eccentricity orbits can be obtained from the Hill-Clohessy-Wiltshire (HCW)[12] model, which is the most elemen-

tary relative motion model in a gravitational field. It assumes a circular reference orbit, a linearized differential gravitational acceleration, and spherical Earth. References 13 and 14 extend the model to account for low eccentricities and higher-order differential gravity terms. The J_2 perturbation results in secular growth in some of the orbital elements, thereby causing drift in relative motion. This drift can be eliminated in the mean sense by using two matching constraints for small orbital element differences, resulting in J_2-invariant orbits.[15] However, the relative orbits obtained by such a technique may not be suitable for some missions. As an alternative, a rate-matching constraint has been developed in Ref. 16 that keeps the along-track motion bounded in the presence of J_2.

This paper first presents the kinematic model for satellite motion and derives a Lyapunov-based feedback control law for orbital transfer. The control law takes into account modeled disturbances. Global, asymptotic stability is shown by the use of LaSalle's theorem. The application of this control law is shown to the particular cases of orbit transfer where the initial or target orbit may have an associated singularity (in terms of orbital elements), and to formation reconfiguration. In both the cases, gain-selection procedures are proposed that are able to reduce control requirements close to their optimal values. When large radius changes are involved, a method is proposed for tracking a spiral trajectory between the initial and desired orbits, generated by using a circumferential thrust assumption. The effect of neglecting J_2 on the performance of the controller is analyzed theoretically as well as numerically. All the developments are supported by numerical examples.

Kinematic Model for Satellite Motion

Frames of Reference

Two frames of reference are considered: 1) The Earth-Centered Inertial (ECI) frame, denoted by $\mathcal{N}$, with basis $\mathcal{B}_N = \{\mathbf{i}_X \quad \mathbf{i}_Y \quad \mathbf{i}_Z\}$. The vector $\mathbf{i}_X$ lies in the equatorial plane, along the line of the equinoxes, the vector $\mathbf{i}_Z$ is aligned with the North Pole, and $\mathbf{i}_Y = \mathbf{i}_Z \times \mathbf{i}_X$. 2) The Local-Vertical-Local-Horizontal (LVLH) frame, denoted by

$\mathcal{L}$ for each spacecraft, with basis $\mathcal{B}_L = \{\mathbf{i}_r \quad \mathbf{i}_\theta \quad \mathbf{i}_h\}$. The vector $\mathbf{i}_r$ lies along the radius vector from the center of the Earth to the spacecraft, $\mathbf{i}_h$ is normal to the plane defined by the position and velocity vectors of the spacecraft, and $\mathbf{i}_\theta = \mathbf{i}_h \times \mathbf{i}_r$. A vector in $\mathcal{N}$ can be transformed into $\mathcal{L}$ through the direction cosine matrix $\mathbf{C}$. This matrix can either be characterized by an Euler 3-1-3 rotation,[17] using the right ascension Ω, inclination i, and argument of latitude θ, or by Euler parameters $\beta_{0\ldots3}$. For any orbit, $\theta = \omega + f$, where ω is the argument of perigee and f is the true anomaly.

Equations of Motion

If the position vector of the spacecraft in $\mathcal{L}$ is $\mathbf{r} = r\mathbf{i}_r$, the inertial acceleration expressed in $\mathcal{B}_L$ is:

$$\begin{aligned}
\ddot{\mathbf{r}} &= \frac{d^2\mathbf{r}}{dt^2} + 2\boldsymbol{\omega} \times \frac{d\mathbf{r}}{dt} + \dot{\boldsymbol{\omega}} \times \mathbf{r} + \boldsymbol{\omega} \times \boldsymbol{\omega} \times \mathbf{r} \\
&= \left[\ddot{r} - \left({\omega_h}^2 + {\omega_\theta}^2\right) r\right] \mathbf{i}_r + \left[\dot{\omega}_h r + 2\omega_h \dot{r} + \omega_r \omega_\theta r\right] \mathbf{i}_\theta \\
&\quad + \left[-\dot{\omega}_\theta r - 2\omega_\theta \dot{r} + \omega_r \omega_h r\right] \mathbf{i}_h \\
&= u_r \mathbf{i}_r + u_\theta \mathbf{i}_\theta + u_h \mathbf{i}_h - \frac{\mu}{r^2} \mathbf{i}_r = \mathbf{u} + \mathbf{g} \qquad (1)
\end{aligned}$$

where, $\mathbf{u} \in \mathbb{R}^3$ is the control applied on the spacecraft, expressed in $\mathcal{B}_L$, $\mathbf{g}$ is the two-body gravitational attraction, and $\boldsymbol{\omega} = \omega_r \mathbf{i}_r + \omega_\theta \mathbf{i}_\theta + \omega_h \mathbf{i}_h$, is the inertial angular velocity vector expressed in $\mathcal{B}_L$. Reference 17 provides detailed description of the angular velocity in terms of either the EPs or Euler angles, and their respective rates. It is also shown in Ref. 8 that an osculation constraint exists such that $\omega_\theta = 0$. Thus, for the complete characterization of an orbit, the seven states $\{r \quad \dot{r} \quad \omega_h \quad \beta_{0\ldots3}\}^T$ are required, with $\sum \beta_i^2 = 1$. The angular velocity about $\mathbf{i}_r$ is determined by setting $\omega_\theta = \dot{\omega}_\theta = 0$ in the h-component of $\ddot{\mathbf{r}}$ in Eq. (1):

$$\omega_r = \frac{u_h}{r\omega_h} \qquad (2)$$

If the external force in the orbit normal direction is zero, then $\omega_r = 0$.

For physical insight into the states of the kinematic model, it must first be stated

that the quantities described above are always defined, irrespective of $e = 0$ or $i = 0$. The significance of r and $\dot{r}$ are obvious; ω_h is equal to h/r^2 where h is the angular momentum of the spacecraft. Furthermore, from Ref. 17 (using $\theta = \omega + f$),

$$\begin{aligned} \beta_0 &= \cos\frac{i}{2}\cos\frac{\Omega+\theta}{2} \qquad \beta_1 = \sin\frac{i}{2}\cos\frac{\Omega-\theta}{2} \\ \beta_2 &= \sin\frac{i}{2}\sin\frac{\Omega-\theta}{2} \qquad \beta_3 = \cos\frac{i}{2}\sin\frac{\Omega+\theta}{2} \end{aligned} \tag{3}$$

The EPs are similar in many respects the equinoctial elements. For example, if $i = 0$, then $\Omega+\omega$ (or $\Omega+\theta$) is defined, but Ω and ω (or θ) cannot be determined independent of each other. In the above expression, it is observed that in such a case, $\beta_1 = \beta_2 = 0$, and $\beta_0 = \cos(\Omega+\theta)/2$ and $\beta_1 = \sin(\Omega+\theta)/2$.

The direction cosine matrix that transforms a vector in $\mathcal{N}$ into one in $\mathcal{L}$, is composed using EPs:

$$\mathbf{C} = \begin{bmatrix} \beta_0^2+\beta_1^2-\beta_2^2-\beta_3^2 & 2(\beta_1\beta_2+\beta_0\beta_3) & 2(\beta_1\beta_3-\beta_0\beta_2) \\ 2(\beta_1\beta_2-\beta_0\beta_3) & \beta_0^2-\beta_1^2+\beta_2^2-\beta_3^2 & 2(\beta_2\beta_3+\beta_0\beta_1) \\ 2(\beta_1\beta_3+\beta_0\beta_2) & 2(\beta_2\beta_3-\beta_0\beta_1) & \beta_0^2-\beta_1^2-\beta_2^2+\beta_3^2 \end{bmatrix} \tag{4}$$

A Lyapunov Approach to Orbital Transfer

In this section, a continuous control law for orbital transfer is discussed. It is assumed that the spacecraft is a point mass, and measurement and actuator errors are neglected. Let $\boldsymbol{\beta}$ denote the EPs for the spacecraft's current position. The acceleration vector of the spacecraft in $\mathcal{B}_L$, from Eq. (1), is equal to the external forces in $\mathcal{B}_L$, i.e., $\ddot{\mathbf{r}} = \mathbf{u} + \mathbf{d}$, where $\mathbf{u} \in \mathbb{R}^3$ is the control acceleration and $\mathbf{d} \in \mathbb{R}^3$ is modeled-disturbance vector. For example, the J_2-induced disturbances[9] are:

$$\mathbf{d} = \begin{Bmatrix} d_r \\ d_\theta \\ d_h \end{Bmatrix} = -\frac{3}{2}\frac{J_2\mu R_e^2}{r^4}\begin{Bmatrix} 1-12(\beta_1\beta_3-\beta_0\beta_2)^2 \\ 8(\beta_1\beta_3-\beta_0\beta_2)(\beta_0\beta_1+\beta_2\beta_3) \\ 4(1-2\beta_1^2-2\beta_2^2)(\beta_0\beta_1+\beta_2\beta_3) \end{Bmatrix} \tag{5}$$

where $J_2 = 1.082629 \times 10^{-3}$, and with EPs substituted for the Euler angles i and θ. The $\mathbf{i}_r$ component of angular velocity $\boldsymbol{\omega}$ is thus $\omega_r = (u_h + d_h)/(\omega_h r)$.

Let $\boldsymbol{\beta}_{\text{des}}$ denote the desired EPs for the spacecraft. Then the Error EPs, denoted by $\boldsymbol{\Delta\beta}$, characterize the current orientation of $\mathcal{B}_L$ with respect to its desired orientation. The Error, desired, and current EPs are related by the following:[17]

$$\begin{Bmatrix} \Delta\beta_0 \\ \Delta\beta_1 \\ \Delta\beta_2 \\ \Delta\beta_3 \end{Bmatrix} = \begin{bmatrix} \beta_0 & \beta_1 & \beta_2 & \beta_3 \\ \beta_1 & -\beta_0 & -\beta_3 & \beta_2 \\ \beta_2 & \beta_3 & -\beta_0 & -\beta_1 \\ \beta_3 & -\beta_2 & \beta_1 & -\beta_0 \end{bmatrix} \begin{Bmatrix} \beta_{\text{des}_0} \\ \beta_{\text{des}_1} \\ \beta_{\text{des}_2} \\ \beta_{\text{des}_3} \end{Bmatrix} \tag{6}$$

The kinematic equations that relate the $\boldsymbol{\Delta\beta}$ to the relative angular velocity are"

$$\begin{Bmatrix} \Delta\dot{\beta}_0 \\ \Delta\dot{\beta}_1 \\ \Delta\dot{\beta}_2 \\ \Delta\dot{\beta}_3 \end{Bmatrix} = \frac{1}{2} \begin{bmatrix} 0 & -\Delta\omega_r & -\Delta\omega_\theta & -\Delta\omega_h \\ \Delta\omega_r & 0 & \Delta\omega_h & -\Delta\omega_\theta \\ \Delta\omega_\theta & -\Delta\omega_h & 0 & \Delta\omega_r \\ \Delta\omega_h & \Delta\omega_\theta & -\Delta\omega_r & 0 \end{bmatrix} \begin{Bmatrix} \Delta\beta_0 \\ \Delta\beta_1 \\ \Delta\beta_2 \\ \Delta\beta_3 \end{Bmatrix} \tag{7}$$

where $\boldsymbol{\Delta\omega}$ is the inertial angular velocity of the current $\mathcal{L}$ frame with respect to its desired orientation, expressed in $\mathcal{B}_L$. That is,

$$\boldsymbol{\Delta\omega} = \boldsymbol{\omega} - \mathbf{C}_{\text{rel}}\boldsymbol{\omega}_{\text{des}} \tag{8}$$

$$\mathbf{C}_{\text{rel}} = \mathbf{C}(\boldsymbol{\beta})\mathbf{C}^T(\boldsymbol{\beta}_{\text{des}}) = \mathbf{C}(\boldsymbol{\Delta\beta}) \tag{9}$$

The Lyapunov Function for General Orbit Transfers

Let the subscript 'des' denote the states corresponding to the desired trajectory. If the desired trajectory is a natural (thrust-free) solution to the two-body problem, then the quantities $\ddot{r}_{\text{des}}$ and $\dot{\omega}_{\text{des}_h}$ can be obtained by using the desired states in Eq. (1). In this case, no control action is required to maintain the desired states after the orbit has been established. On the other hand, if the desired states do not correspond to a Keplerian orbit, and evolve with time according to specified equations, thrust will be

required to maintain the required motion. The modeled disturbance for the desired trajectory can also be determined in terms of the desired states.

Let $\mathbf{z} = \begin{Bmatrix} \boldsymbol{\Delta\beta}^T & \Delta'\omega_h & \Delta r & \Delta\dot{r} \end{Bmatrix}^T \in Z = \mathbb{S}^3 \times X$, where $\mathbb{S}^3$ is the 3-sphere, and $X \subset \mathbb{R}^3$. The errors $\Delta'\omega_r$ and $\Delta'\omega_h$ are the components of the direct difference between the current and desired angular velocity vectors, $\boldsymbol{\Delta'\omega} = \boldsymbol{\omega} - \boldsymbol{\omega}_{\text{des}}$. In general, $\boldsymbol{\Delta'\omega} \neq \boldsymbol{\Delta\omega}$. Obviously, $\Delta'\omega_\theta = 0$, due to the osculation constraint. The last two terms in $\mathbf{z}$ correspond to the error between the current and desired radial distance, and current and desired radial velocity, respectively. The Lyapunov function, $V : Z \longrightarrow \mathbb{R}_{\geq 0}$, is defined as the following:

$$V = (1 - \Delta\beta_0)^2 + \widetilde{\boldsymbol{\Delta\beta}}^T \widetilde{\boldsymbol{\Delta\beta}} + \frac{K_1}{2}\Delta'\omega_h^2 + \frac{K_2}{2}\Delta r^2 + \frac{K_3}{2}\Delta\dot{r}^2 \tag{10}$$

where $K_i \in \mathbb{R}^+$, and $\widetilde{\boldsymbol{\Delta\beta}} = \{\Delta\beta_1 \ \Delta\beta_2 \ \Delta\beta_3\}^T$ is the reduced error EP set. When the current LVLH frame aligns with the desired LVLH frame, $\boldsymbol{\Delta\beta} = \{1 \quad 0 \quad 0 \quad 0\}^T$, and all the other error states are zero. This is the desired equilibrium, denoted by $\mathbf{z}_{\text{eq}}$, and it is clear that $V(\mathbf{z}_{\text{eq}}) = 0$ and $V(\mathbf{z}) > 0 \ \forall \mathbf{z} \in Z \backslash \{\mathbf{z}_{\text{eq}}\}$.

A control law that asymptotically stabilizes the current orbit with respect to the desired orbit can be obtained by taking the time derivative of the Lyapunov function:

$$\dot{V} = -2\Delta\dot{\beta}_0 + K_1\Delta'\omega_h\Delta'\dot{\omega}_h + K_2\Delta r\Delta\dot{r} + K_3\Delta\dot{r}\Delta\ddot{r} \tag{11}$$

where $\Delta\ddot{r} = \ddot{r} - \ddot{r}_{\text{des}}$. The reduced EP set is an eigenvector of the corresponding direction cosine matrix. Consequently, $\mathbf{C}_{\text{rel}}\widetilde{\boldsymbol{\Delta\beta}} = \mathbf{C}_{\text{rel}}^T\widetilde{\boldsymbol{\Delta\beta}} = \widetilde{\boldsymbol{\Delta\beta}}$, and it follows that $\boldsymbol{\Delta\omega}^T\widetilde{\boldsymbol{\Delta\beta}} = \boldsymbol{\Delta'\omega}^T\widetilde{\boldsymbol{\Delta\beta}}$. Using this relation in Eq. (11):

$$\dot{V} \ = \ \Delta'\omega_r\Delta\beta_1 + \Delta'\omega_h\left(\Delta\beta_3 + K_1\Delta'\dot{\omega}_h\right) + \Delta\dot{r}\left(K_2\Delta r + K_3\Delta\ddot{r}\right) \tag{12}$$

To ensure $\dot{V}(\mathbf{z}) \leq 0 \ \forall \mathbf{z} \in Z$ the following substitutions are made:

$$\Delta'\omega_r \ = \ \omega_r - \omega_{\text{des}_r} = -K_4\Delta\beta_1 \tag{13a}$$

$$K_1\Delta'\dot{\omega}_h \ = \ K_1\left(\dot{\omega}_h - \dot{\omega}_{\text{des}_h}\right) = -K_5\Delta'\omega_h - \Delta\beta_3 \tag{13b}$$

$$K_3\Delta\ddot{r} \;=\; -K_6\Delta\dot{r} - K_2\Delta r \tag{13c}$$

with $K_{4\ldots6} \in \mathbb{R}^+$. For convenience, one may set $c_1 = K_6/K_3$, $c_2 = K_2/K_3$, $c_3 = K_5/K_1$, $c_4 = 1/K_1$, and $c_5 = K_4$. Equations (13), along with Eq. (1) with the explicit disturbing modeling (replacing $\mathbf{u}$ with $\mathbf{u}+\mathbf{d}$), lead to the following control laws that stabilize the system about the origin:

$$u_r \;=\; -c_1\Delta\dot{r} - c_2\Delta r - \omega_h^2 r + \frac{\mu}{r^2} - d_r + \ddot{r}_{\text{des}} \tag{14a}$$

$$u_\theta \;=\; -c_3\Delta'\omega_h r - c_4\Delta\beta_3 r + 2\omega_h\dot{r} - d_\theta + \dot{\omega}_{\text{des}_h} r \tag{14b}$$

$$u_h \;=\; -c_5\Delta\beta_1\omega_h r - d_h + w_{\text{des}_r}\omega_h r_h \tag{14c}$$

By substituting Eqs. (13) in Eq. (12), the time derivative of the Lyapunov reduces to

$$\dot{V} = -K_4\Delta\beta_1^2 - K_5\Delta'\omega_h^2 - K_6\Delta\dot{r}^2 \tag{15}$$

It is not immediately obvious that $\dot{V}(\mathbf{z}) < 0\ \forall\mathbf{z} \in Z\backslash\{\mathbf{z}_{\text{eq}}\}$. Asymptotic stability of the system is shown using LaSalle's Theorem, and is presented in the appendix.

It is noted from Eq. (15) that the gains $K_{4\ldots6}$ are incorporated to ensure $\dot{V}(\mathbf{z}) \leq 0$, and while are positive, are not restricted to being constant. Consequently, the gains c_1, c_3, and c_5 can be selected to be time-varying and positive, without affecting stability. Such an approach has been used in Ref. 5. References 5 and 18 use the structure of Gauss' equations to obtain locations for velocity increment application in the impulsive control problem. For example, it is well-known that for low-eccentricity transfers, out-of-plane corrections should be performed when the two orbits cross at their common nodes. This is directly reflected in the u_h component of the control law. In terms of orbital elements, the latitude of common node crossing is given by $\tan\theta_{\text{des}} = \Delta\Omega\sin i_{\text{des}}/\Delta i$. For small angular differences, it can be shown that:

$$\Delta\beta_0 \approx 1, \quad \Delta\beta_1 \approx \frac{\Delta i}{2}\cos\theta_{\text{des}} + \frac{\Delta\Omega}{2}\sin i_{\text{des}}\sin\theta_{\text{des}} \tag{16}$$

$$\Delta\beta_2 \approx -\frac{\Delta i}{2}\sin\theta_{\text{des}} + \frac{\Delta\Omega}{2}\sin i_{\text{des}}\cos\theta_{\text{des}}, \quad \Delta\beta_3 \approx \frac{\Delta\theta}{2} + \frac{\Delta\Omega}{2}\cos i_{\text{des}}$$

Thus, to first approximations the crossing of common nodes occurs when $\Delta\beta_2 = 0$, or when $\Delta\beta_1$ takes an extreme value, since $d\Delta\beta_1/d\theta_{\text{des}} = \Delta\beta_2$. Since Eq. (15) has $\Delta\beta_1^2$ as a term, its contribution to $\dot{V}$ is highest at this point. Thus, out-of-plane control is best applied when $\Delta\beta_2 = 0$. This is under the assumption that $\omega_h r$ (velocity in the along-track direction) is nearly constant, which is true for near-circular orbits. For highly eccentric orbits, $r\omega_h$ is the smallest at application points near the apogee; this implies that proper out-of-plane control application points will be close to the apogee.[19] Thus the gains can be adjusted accordingly, depending on which quantity takes priority and the type of transfer desired.

Applications to Transfers to Large Orbits

While the control law derived in the previous section can be used for any transfer, a level of sub-optimality can be achieved by using the physical characteristics of the problem effectively. Spencer and Culp[20] develop a method for orbital transfer from a parking orbit to MEO/GEO by using equinoctial elements, and by dividing the problem into different stages. The primary motivation behind the staging algorithm in this problem is that if initial errors are very large (as is the case for transfers involving large changes), then the initial acceleration levels demanded by the controller will be very large. Not only does this result in higher control requirements, it is also possible that constraints on thruster design may limit the availability of such thrust levels. Furthermore, seeing that the out-of-plane problem can be treated separate from the in-plane problem, it is more economical to make inclination or right ascension changes in the larger of the initial or final orbit, since velocity levels are lower in larger orbits. Therefore, the problem of transferring to a large orbit can be divided into two parts: 1) in-plane control law transferring the spacecraft outwards following a spiral reference trajectory to the desired orbit, and 2) generalized control law to bring the spacecraft to its desired final states. The first stage is studied in greater detail.

Reference Trajectories for In-Plane Transfer

In the first stage, it is desired to move the satellite slowly outwards until it reaches the radial distance of the desired orbit. This 'transfer orbit' is obtained by tracking the following approximate solution arising as a result of constant, low, circumferential thrust:[21,22]

$$r(t) = r_0 \left(1 - \frac{\bar{u}_\theta t}{v_0}\right)^{-2} \tag{17a}$$

$$\theta(t) = \theta_0 + \frac{v_0^2}{4 r_0 \bar{u}_\theta} \left[1 - \left(1 - \frac{\bar{u}_\theta t}{v_0}\right)^4\right] \tag{17b}$$

where $\bar{u}_\theta$ is the constant circumferential thrust and v_0 is the velocity corresponding to the initial circular orbit. The quantity θ is defined for zero eccentricities. If initial inclination is also zero, then $\theta + \Omega$ should be used instead of θ in Eq. (17b). An attempt is made to reduce the phasing required once the radial distance of the target orbit, r_f, has been reached. This is made possible if the final argument of latitude, θ_f of the transfer trajectory, is the same as, or as close as possible to, the argument of latitude of the desired trajectory, which is obtained from the desired EPs. Thus, given t_f, r_f and θ_f, the quantities $\bar{u}_\theta$, and θ_0 can be determined uniquely from Eqs. (17a) and (17b). In the event the final orbit is non-circular, r_f and θ_f should correspond to the desired orbit's apogee. This is desired so that the terminal control law initiates in a region where the velocity is low, as opposed to region where the velocity is high. Navigational errors are also smaller at apogee than at perigee because of the rapid change in system states in the latter region.

It is now assumed that the maneuver of the spacecraft starts at the point on its initial orbit, where $\theta = \theta_0$. This does not affect stability of the control law since only the initial conditions of the system change. For zero initial eccentricities, as is assumed in Ref. 21, r_0 is constant, but for low eccentricities, at this value of θ_0, the radius also changes. Consequently, Eqs. (17a) and (17b) are solved iteratively using the r_0 corresponding to the updated θ_0, until θ_0 and $\bar{u}_\theta$ converge to within a predefined tolerance. The first quantity is used to define the initiation point of the control, and

the second quantity is a shaping parameter for the reference transfer trajectory.

In-Plane Tracking of the Reference Trajectory

From Eqs. (17a) and (17b), and their higher derivatives, the quantities r_{des}, $\dot{r}_{\text{des}}$, $\ddot{r}_{\text{des}}$, ω_{des_h} and $\dot{\omega}_{\text{des}_h}$ are obtained as functions of time. Tracking of this in-plane trajectory is performed by using a modified form of Eq. (10), without the error Euler parameter terms. Therefore, the new Lyapunov function $V_{\text{ip}} : X \longrightarrow \mathbb{R}_{\geq 0}$, is defined as:

$$V_{\text{ip}}(\widetilde{\mathbf{z}}) = \frac{K_1}{2}\Delta'\omega_h^2 + \frac{K_2}{2}\Delta r^2 + \frac{K_3}{2}\Delta\dot{r}^2 \tag{18}$$

where $\widetilde{\mathbf{z}}$ only comprises the radial, radial velocity and out-of-plane component of angular velocity errors. It can be shown that control laws to render $\dot{V}_{\text{ip}}$ negative definite can be obtained trivially from Eq. (14), by setting $c_4 = c_5 = 0$, and the only equilibrium is $\omega_h = \omega_{\text{des}_h}$, $r = r_{\text{des}}$, and $\dot{r} = \dot{r}_{\text{des}}$, as desired.

Gain Selection

In the transfer stage, high values for c_3 need to be selected to control the ω_h error. The analysis in Ref. 21 assumes that the radial thrust is negligible, and centripetal acceleration $\omega_h^2 r$ is nearly equal to gravitational attraction μ/r^2. If ω_h errors are not reduced quickly, this results in added radial control, increasing the total control requirement.

In the second stage, choices for gains can be made by studying the dynamics of the closed-loop system. By substituting Eq. (14) in Eq. (1), the following equations are obtained.

$$\Delta\ddot{r} + c_1\Delta\dot{r} + c_2\Delta r = 0 \tag{19a}$$

$$\Delta'\dot{\omega}_h + c_3\Delta'\omega_h + c_4\Delta\beta_3 = 0 \tag{19b}$$

$$\Delta'\omega_r + c_5\Delta\beta_1 = 0 \tag{19c}$$

From the radial equation, judicious choices for the gains are $c_2 = \mathcal{O}(n^2)$ and $c_1 =$

$2\sqrt{c_2}$, where n is a natural frequency that is governed by the desired time of convergence, and can be taken to be the mean motion of the target orbit. Similar analysis can be performed on the attitude equations, with the small angular difference assumptions in Eq. (16). Then, it can be shown that $\Delta'\omega_h \approx 2\Delta\dot{\beta}_3$. The third of the closed-loop equations is coupled with $\Delta\beta_2$, and consequently yields, $\Delta\ddot{\beta}_1 + c_5\Delta\dot{\beta}_1 + n^2\Delta\beta_1 = 0$. Therefore, for these cases, $c_4/2 = \mathcal{O}(n^2)$, and $c_3 = \sqrt{(2c_4)}$. To encourage out-of-plane control application at locations where $\Delta\beta_2 = 0$, a time-varying gain such as $c_5 = c_{50}e^{-k|\Delta\beta_2|}, k > 0$, is used. The maximum value can be chosen from the small angular difference assumptions, or $c_{50} \approx 2n$. These provide excellent initial guesses for the gains to be used in the control law, even when applied to the problem of formation reconfiguration. Further tuning of the gains becomes necessary if the mission requirements change; for example, a faster transfer will require a higher natural frequency of the closed-loop system.

Applications to Formation Reconfiguration

Relative Motion and Initial Conditions

The HCW equations[12] are a set of three, second-order, linear differential equations that govern the motion of a Deputy satellite relative to the Chief satellite, in the LVLH frame of the Chief, with x, y, and z as the relative positions along the radial, along-track and normal directions. The HCW initial conditions are those that do not allow secular along-track growth. In particular, projected circular orbits (PCO) have the following solution:

$$x = \frac{\rho}{2}\sin(n_C t + \alpha_0) \tag{20a}$$

$$y = \rho\cos(n_C t + \alpha_0) \tag{20b}$$

$$z = \rho\sin(n_C t + \alpha_0) \tag{20c}$$

where, ρ is the relative orbit radius, and α_0 is the initial phase angle. ρ and α_0 are shown with respect to the LVLH frame of the Chief in Fig. 1. Vadali et al.[16] derived differential orbital elements corresponding to the PCO conditions, by linearizing the

direction cosine matrix of the Deputy with respect to that of the Chief. With the additional use of the rate-matching constraint to account for J_2 effects, initial orbital element differences valid for very low eccentricity reference orbits can be obtained as shown:

$$\delta a = \frac{1}{2} J_2 \left(\frac{R_e^2}{a_C}\right) \frac{(3\eta + 4)}{\eta^4} \left[-(1 - 3\cos^2 i_C) \frac{e_C}{\eta^2} \delta e - \sin 2i_C \delta i \right] \tag{21a}$$

$$\delta e = -\frac{\rho}{2a_C} \sin(\omega_C + \alpha_0) \tag{21b}$$

$$\delta i = \frac{\rho}{a_C} \cos \alpha_0 \tag{21c}$$

$$\delta \Omega = -\frac{\rho}{a_C} \frac{\sin \alpha_0}{\sin i_C} \tag{21d}$$

$$\delta \omega = -\frac{\rho}{2a_C e_C} \cos(\omega_C + \alpha_0) + \frac{\rho}{a_C} \frac{\cos i_C \sin \alpha_0}{\sin i_C} \tag{21e}$$

$$\delta M = \frac{\rho}{2a_C e_C} \cos(\omega_C + \alpha_0) \tag{21f}$$

where, $\eta = \sqrt{(1 - e_C^2)}$, and the subscript C denotes elements of the Chief. Similarly, the subscript D will denote the elements of the Deputy.

The condition on δa corresponds to the period-matching condition in Ref. 16. In the absence of J_2, this would be zero to ensure no drift between the Deputy and Chief. The rest of the elemental differences correspond to the PCO requirement.

It should be noted that the differential elements may be expressed in characterizations other than classical orbital elements. For example, Ref. 15 provides initial orbit differences using Delauney elements, while Ref. 18 characterizes such differences using nonsingular elements. Irrespective of the characterization, conversion from any of the orbital element sets to kinematic states is straightforward and without singularities.

Simplification the Control Law

It is evident that the control components specified in Eqs. (14) require knowledge of the elements at every instant. In the absence of perturbations, the desired trajectory can be propagated analytically from the initial conditions. If the J_2 perturbation is included, then simulations also show that mean elements can be used to analytically

propagate the desired orbit, though at this point it is not possible to show in what region the errors lie. The use of mean elements enables the treatment of a, e, and i as constants, and the right ascension, argument of perigee, and mean anomaly as linear functions of time.

More importantly, it can be observed that the modeled disturbance accelerations in Eqs. (14) are expressed as the differences between their current values and desired values. For cases involving J_2, considerable simplification of the control law is possible by dropping these terms. Appendix B studies the effects of such an action.

Correct Position for Initiating the Control

As will be shown in the numerical simulations, initiating the control at arbitrary points leads to excessive control acceleration. By seeking positions where the control requirement is minimal, one can aim to reduce the total control requirement for the reconfiguration. This is especially useful for formation reconfiguration, since it is assumed that the Deputy is already in a regular formation about the Chief, and consequently, does not drift too far from this region. Furthermore, it is assumed that the control is active throughout, once initiated. Initiating the control at a point other than $t = 0$ has no effect on the stability of the law, since it only changes the initial conditions.

Low-Eccentricity Reference Orbit

By using the small angular difference approximations, the condition for best use of an out-of-plane control correspond to $\Delta\beta_2 = 0$. Thus, the appropriate value of the Deputy's argument of latitude, $\theta_{D_{\text{appl}}}$, for initiating control, is given by:

$$\theta_{D_{\text{appl}}} = \tan^{-1}\left(\frac{\Delta\Omega \sin i_D}{\Delta i}\right) \tag{22}$$

From Eq. (21),

$$\Delta\Omega = \delta\Omega_{\text{final}} - \delta\Omega_{\text{initial}} = -\frac{1}{a_C \sin i_C}\left(\rho_f \sin\alpha_{0_f} - \rho_i \sin\alpha_{0_i}\right) \tag{23a}$$

$$\Delta i \;=\; \delta i_{\text{final}} - \delta_{\text{initial}} = \frac{1}{a_C}\left(\rho_f \cos\alpha_{0_f} - \rho_i \cos\alpha_{0_i}\right) \tag{23b}$$

Substituting Eqs. (23) in Eq. (22), the following expression is obtained:

$$\theta_{D_{\text{appl}}} = \omega_D + f_{D_{\text{appl}}} = \tan^{-1}\left[-\left(\frac{\sin i_D}{\sin i_C}\right)\left(\frac{\rho_f \sin\alpha_{0_f} - \rho_i \sin\alpha_{0_i}}{\rho_f \cos\alpha_{0_f} - \rho_i \cos\alpha_{0_i}}\right)\right] \tag{24}$$

Equation (24) has two solutions, corresponding to each nodal crossing. Without loss of generality, the one closest to epoch is selected.

It will be shown in the numerical simulations that the initiation of control at a true anomaly of $f_{D_{\text{appl}}}$ shows lower TCR than an initiation anywhere else.

High-Eccentricity Reference Orbit or the Most General Case

For formations where the eccentricity of the reference orbit is very high, the approach in the previous section is no longer valid. This is because, the magnitude of control required in the orbit normal direction is much less than that required in the radial and circumferential directions. The position for minimal control in the orbit normal direction, therefore, does not necessarily imply a minimum for the magnitude of the total control. Furthermore, for very high eccentricities, Ref. 19 obtains results that indicate that the velocity increments (in the case of a two-impulse optimal control problem) are best applied in the region of the apogee of the Deputy's orbit.

From the observation in the beginning of this section, it is logical to conclude that the control should be initiated at the point where its magnitude is a minimum. To this end, a function Ψ is defined as the following:

$$\Psi \;=\; |\mathbf{u}|^2 = u_r^2 + u_\theta^2 + u_h^2 \tag{25}$$

The appropriate position can be obtained by minimizing Ψ with respect to the eccentric anomaly, i.e., by setting its derivative with respect to E_D to zero. The use of eccentric anomaly as the independent variable is preferred over true anomaly due to the less-complex nature of equations, and is more amenable than the use of time,

due to the increase in rate of change of quantities near the perigee. Neglecting J_2, the three components of control from Eq. (14) are used in Eq. (25). The calculation of their derivatives requires the following expressions:

$$\frac{\partial r_D}{\partial E_D} = a_D e_D \sin E_D \tag{26a}$$

$$\frac{\partial \dot{r}_D}{\partial E_D} = \frac{n_D a_D e_D}{(1 - e_D \cos E_D)^2} (\cos E_D - e_D) \tag{26b}$$

$$\frac{\partial \omega_{D_h}}{E_D} = -\frac{2h_D}{r_D^3} \frac{\partial r_D}{\partial E_D} \tag{26c}$$

$$\frac{\partial \Delta\beta_1}{\partial E_D} = \frac{1}{2}\Delta\beta_2 \left(\frac{df_D}{dE_D} + \frac{df_{D_{\text{des}}}}{dE_{D_{\text{des}}}} \frac{dE_{D_{\text{des}}}}{dE_D} \right) \tag{26d}$$

$$\frac{\partial \Delta\beta_3}{\partial E_D} = \frac{1}{2}\Delta\beta_0 \left(\frac{df_D}{dE_D} - \frac{df_{D_{\text{des}}}}{dE_{D_{\text{des}}}} \frac{dE_{D_{\text{des}}}}{dE_D} \right) \tag{26e}$$

where $df_D/dE_D = \sqrt{1 - e_D^2}/(1 - e_D \cos E_D)$.

The expressions corresponding to the desired states can be obtained in a similar manner, by substituting the desired orbital elements in the above equations. For example,

$$\begin{aligned} \frac{\partial r_{D_{\text{des}}}}{\partial E_D} &= a_{D_{\text{des}}} e_{D_{\text{des}}} \sin E_{D_{\text{des}}} \frac{dE_{D_{\text{des}}}}{dE_D} \\ \frac{dE_{D_{\text{des}}}}{dE_D} &= \frac{dE_{D_{\text{des}}}}{dt} \Big/ \frac{dE_D}{dt} = \frac{n_{D_{\text{des}}}}{n_D} \frac{(1 - e_D \cos E_D)}{(1 - e_{D_{\text{des}}} \cos E_{D_{\text{des}}})} \end{aligned} \tag{27}$$

The inverse solution to Kepler's equation, $M_{D_{\text{des}}} = E_{D_{\text{des}}} - e_{D_{\text{des}}} \sin E_{D_{\text{des}}}$, is used to evaluate $E_{D_{\text{des}}}$. Since eccentricity expansions can only be used when the eccentricity of an orbit is less than 0.6627,[22] Kepler's equation needs to be solved iteratively. It should be noted that $e_{D_{\text{des}}}$ is a constant, and $M_{D_{\text{des}}} = M_C + \delta M$, where δM is constant. The mean anomaly of the Chief can be obtained by solving Kepler's equation directly from E_C, which is obtained from the following equations:

$$\frac{dE_C}{dE_D} = \frac{n_C}{n_D} \frac{(1 - e_D \cos E_D)}{(1 - e_C \cos E_C)} \tag{28}$$

$$E_C \approx E_{C_0} + \left. \frac{dE_C}{dE_D} \right|_{E_C = E_D} (E_D - E_{D_0}) \tag{29}$$

The approximation shown above allows the treatment of $dE_{D_{\text{des}}}/dE_D$ and $E_{D_{\text{des}}}$ as nonlinear functions of E_D alone, since the other quantities in Eq. (27) are constants for the given orbit of the Chief and the initial orbit of the Deputy. Equations (27)-(29) can be used with Eq. (26), and the corresponding equations for the desired states and their derivatives, to evaluate the minimum of Eq. (25). Thus, $\Psi = \Psi(E_D)$ only; its zeros, given by $E_{D_{\text{appl}}}$, can be obtained by any numerically iterative procedure. For cases with high-eccentricity reference orbits, acceptable values are in the region of the apogee; therefore, $E_{D_{\text{appl}}} = \pi$ can be used as an initial guess. If the initial time corresponds to the perigee location, then values that are less than π are preferred over those that are greater than π, due to the time of operation.

Numerical Simulations

Orbital Transfer

Herman and Spencer[23] obtain open-loop optimal solutions using continuous thrust for various cases of LEO to MEO and LEO to GEO transfer, using different levels of constant thrust. An example from Ref. 23 is used as a means of comparing the developed control law with existing literature. The transfer considered is one from a parking orbit of semimajor axis $7,003\,\text{km}$, eccentricity 0.005, and inclination 30° (other elements zero), to a circular MEO of radius $26,560\,\text{km}$ and inclination 54.7° (other elements zero), and is shown in Fig. 2. While the models include the perturbations due to J_2, the control laws do not. The nominal time for transfer from the LEO to the planar MEO is chosen to be three days. For the transfer stage, the gains are chosen as $c_3 = 0.1$, $c_2 = 1 \times 10^{-5}$, and $c_1 = \sqrt{(2c_2)}$. For the second stage, the gains are chosen as $c_1 = c_3 = 4 \times 10^{-4}$, $c_2 = 4 \times 10^{-8}$, and $c_4 = 8 \times 10^{-8}$. The gain $c_5 = 4 \times 10^{-4} e^{-100|\Delta\beta_2|}$. The generation of the reference spiral trajectory from Eqs. (17a) and (17b) results in $\bar{u}_\theta = 2.12 \times 10^{-2}\,\text{m/s}^2$, and θ_0 of 135.92°. That is, control is initiated approximately 92 minutes after the beginning of the simulation. Figure 3 shows the control profile for this transfer. It is observed that u_θ for the transfer stage is approximately $2.02 \times 10^{-2}\,\text{m/s}^2$, which is very close to the predicted value. Furthermore, an initial radial control is required to bring the spacecraft to the

spiralling reference, which reduces to near-zero almost immediately. Though the control appears impulse-like due to the scale of time on the x-axis, it is actually applied over a period of 15-20 minutes. In the second stage, most of the control is applied for inclination change, and due to the nature of the gain c_5, is selectively applied when the spacecraft crosses the line of nodes.

The total control requirement (TCR) uses the single thruster assumption and calculates the integral of the 2-norm of the control vector. It is thus analogous to Δv for impulsive maneuvers. The TCR for this maneuver is shown in Fig. 4, and is approximately 6.5 km/s. The second stage of the transfer is terminated once the radial error is less than 10cm and the reduced error EPs are smaller than 1×10^{-5}, and the total transfer takes approximately 5 days. The open-loop optimal transfer in Ref. 23 does not include control of the position on the desired orbit, and using a constant thrust of $0.01\,\mathrm{m/s^2}$, transfers to the desired orbit in 5-6 days using a Δv-equivalent of 5.1 km/s. Additional fuel will be required to achieve correct phasing in the orbit. Improved performance of the control law can be achieved using a better reference profile as a well as optimized gain selection.

Low Eccentricity Formation Reconfiguration

A reconfiguration for a formation in low-eccentricity reference orbit is considered. The choice of gains follows from the small angular difference assumptions outlined in the development of the control law. The elements of the Chief's orbit are $\mathbf{e}_C = \{a_C \; e_C \; i_C \; \Omega_{C_0} \; \omega_{C_0} \; M_{C_0}\}^T = \{7100\,\mathrm{km} \; 0.005 \; 70^\circ \; 0^\circ \; 0^\circ \; 0^\circ\}^T$. The initial configuration of the relative orbit has $\rho = 1\,\mathrm{km}$ and $\alpha_0 = 0^\circ$. Figures 5(i) and 5(ii) show the θ-h projection of the reconfiguration to $\rho = 2\,\mathrm{km}, \alpha_0 = 0^\circ$, and the TCR in the presence and absence of J_2. The reconfiguration for the $\alpha_{0_f} = 0^\circ$ case is very similar to the impulsive reconfiguration in Ref. 19, except for the overshoot in the $-y$ direction. The numerical value of the TCR, however, is slightly higher than the total velocity increment required in the two-impulse optimal reconfiguration, presented in Ref. 19, which is approximately 1.1 m/s.

Figure 6 shows the control history for this reconfiguration. The magnitude of the

control requirement is maximum at the beginning of the maneuver, which allows its approximation as a single velocity impulse for the purpose of analysis. If the phase angles of the initial and final configurations are the same, then, letting $\alpha_{0_i} = \alpha_{0_f} = \alpha_0$, it can be shown that Eq. (24) reduces to:

$$\begin{aligned} \tan\theta_{D_{\text{appl}}} &\approx -\tan\alpha_0 \\ \text{or} \quad \theta_{D_{\text{appl}}} &= \pi - \alpha_0 \end{aligned} \tag{30}$$

Figure 7 compares the TCR for three arbitrary cases where the initial and final phase angles are equal. It is observed that the TCR in all three cases have negligible difference. This is achieved by initiating reconfiguration at the appropriate position. Figure 8(i) shows the reconfiguration from the given initial formation, to a formation with $\rho = 2\,\text{km}$ and $\alpha_0 = 90^\circ$. Since $f_{D_{\text{appl}}} \neq 0$, it is observed that the Deputy continues on its initial relative orbit for some time before control is applied. The TCR for this reconfiguration is shown in Fig. 8(ii). It is observed that if the reconfiguration is initiated at $f_D = 0^\circ$, the TCR is approximately $8\,\text{m/s}$. By initiating the reconfiguration at the appropriate location, the TCR is reduced to approximately $3.5\,\text{m/s}$. This is comparable to the total velocity increment of $2.6\,\text{m/s}$, in the impulsive reconfiguration in Ref. 19.

Minimization of the function Ψ in Eq. (25) by finding the zeros of its derivative, yields two minima, which correspond to the analytical expression in Eq. (24), one of which corresponds to the solution from Eq. (24). Thus one can conclude that the more trivial expression derived for low-eccentricity references, is a special case of the general minimization problem posed in Eq. (25).

By initiating the control at the appropriate location, the same set of gains can be used for a large class of low-eccentricity reconfigurations. The Lyapunov function selected does not yield controls for optimal (lowest) fuel consumption; since optimality has not been considered in the derivation. Therefore, control requirements lower than those from the impulsive algorithm in Ref. 19 can never be obtained with the specific structure of the Lyapunov function selected.

High Eccentricity Reference Orbit

The theory used to derive the initial conditions for the PCO is valid only for low eccentricities, since it involves eccentricity expansions of the true anomaly in terms of the mean anomaly, correct only to the first order. Therefore, relative orbits using initial conditions from Eq. (21) in general do not provide circular orbits if the reference orbit eccentricity is high. There is at present, no characterization for such orbits for highly eccentric reference orbits. For the sake of convenience, the orbital element differences in Eq. (21) will be used to in this example.

While all simulations account for the J_2 perturbation, for high eccentricity reconfigurations, the mean element-based control law does not provide adequate performance. It is observed that the simplified model tracks the mean desired elements of the Deputy satellite very well, but when the control is applied to the true system, noticeable drift is seen. It thus becomes necessary to use osculating elements for the desired Deputy trajectory, obtained from integration of the truth model.

The high-eccentricity reconfiguration example chosen has a reference orbit similar to that of the MMS mission, and is characterized by $\mathbf{e}_C = \{42095.70\,\text{km}\ 0.8182\ 50^\circ\ 0^\circ\ 0^\circ\ 0^\circ\}^T$. These orbital elements correspond to an orbit with distances of apogee and perigee, given by $r_a = 12R_e$, and $r_p = 1.2R_e$, respectively. Let the initial formation be characterized by $\rho = 10\,\text{km}$ and $\alpha_0 = 0^\circ$ and let the desired formation be characterized by $\rho = 20\,\text{km}$ and $\alpha_0 = 0^\circ$. Figure 9(i) shows the variation of the function Ψ from Eq. (25), with the true anomaly of the Deputy. The second panel magnifies the region $0.42 \leq f_D/2\pi \leq 0.45$, showing that the minimum of Ψ occurs prior to the apogee. By using the algorithm to find the zeros of Ψ', $f_{D_{\text{appl}}} = 150.27^\circ$. This can also be observed in Fig. 9(ii). Figure 10(i) shows the resulting reconfiguration, and Fig. 10(ii) shows the TCR for this reconfiguration. The TCR in the presence of J_2 is slightly higher. For comparison, the total velocity increment required from the optimal impulsive reconfiguration is approximately $0.6\,\text{m/s}$ for the same reconfiguation. The impulsive reconfiguration performs better, since both impulses are placed symmetrically about the apogee, while the use of continuous control forces some amount of control to be

applied near perigee, increasing the control requirement.

It must be noted that Δv comparison is not quite appropriate as low-thrust propulsion typically is much more efficient in terms of fuel requirement compared to high-thrust propulsion.

Conclusions

This paper presents a novel Lyapunov function-based control law for orbit transfer problems. This control law, motivated by developments in the field of attitude control, is shown to be capable of high performance on a variety of examples, including LEO-MEO transfers and formation reconfiguration in low- and high-eccentricity orbits. For transfers involving large changes in orbit radii, the control law is implemented to track a reference analytical solution. For low-eccentricity reconfigurations, the control law is further simplified by neglecting the differential J_2 acceleration terms in the control design model and by the use of mean elements. An algorithm has been developed, that yields the position at which initiating the control results in the lowest total control requirement for a given control law. This algorithm is applicable to the most general reconfiguration problem. This enables the use of the same set of gains for a whole class of reconfigurations.

Acknowledgments

This research was supported by NASA Grant NAG5-11349 and a grant from the Advanced Technology Program funded by the Texas Board of Higher Education. The authors wish to thank Kyle T. Alfriend for their helpful discussions with him.

Appendix A: Proof of Asymptotic Stability

It has already been shown in Eqs. (10) and (15), that $V(\mathbf{z}) > 0$ and $\dot{V}(\mathbf{z}) \leq 0$ $\forall \mathbf{z} \in Z \backslash \{\mathbf{z}_{\text{eq}}\}$. The set $E = \left\{ \mathbf{z} \in Z | \dot{V}(\mathbf{z}) = 0 \right\}$ contains the points where $\Delta\beta_1 = \Delta'\omega_h = \Delta\dot{r} = 0$. If M is the largest invariant set in E, it needs to be shown that the region M contains only the origin, i.e., when $\Delta\beta_1 = \Delta'\omega_h = \Delta\dot{r} = 0$, all other error

variables are zero.

By substituting the radial control from Eq. (14a) in Eq. (1), the equation $\Delta\ddot{r} + c_1\Delta\dot{r} + c_2\Delta r = 0$ is obtained. For $c_1, c_2 > 0$, the only equilibrium for this system is $\Delta r = \Delta\dot{r} = 0$; consequently, when $\dot{r} = \dot{r}_{\text{des}}$, $r = r_{\text{des}}$.

Since $\Delta'\omega_h = 0$, it follows that $\omega_h = \omega_{\text{des}_h}$. Substituting (14c) in the expression for ω_r, $\omega_r = \omega_{\text{des}_r}$, which, along with the osculation constraint, implies $\boldsymbol{\Delta'\omega} = \mathbf{0}$.

The closed-loop system obtained upon substituting Eq. (14b) in the $\mathbf{i}_\theta$ component of Eq. (1) results in $\Delta\beta_3 = 0$, given that $\Delta'\omega_h = 0$. Since $\Delta\beta_1$ is also zero, it is clear that $\Delta\dot{\beta}_1 = \Delta\dot{\beta}_3 = 0$. Since $\boldsymbol{\Delta\omega}^T\widetilde{\boldsymbol{\Delta\beta}} = \boldsymbol{\Delta'\omega}^T\widetilde{\boldsymbol{\Delta\beta}} = 0$, it follows that $\Delta\dot{\beta}_0 = 0$. Finally, since $\boldsymbol{\Delta\beta}^T\boldsymbol{\Delta\beta} = 1$, differentiating the expression leads to the conclusion that $\Delta\dot{\beta}_2 = 0$. Therefore, $\boldsymbol{\Delta\dot{\beta}} = \mathbf{0} = \boldsymbol{\Delta\omega}$.

Only one of $\Delta\beta_0$ and $\Delta\beta_2$ needs to be determined; the value of the other is fixed by the Euler parameter constraint. By simplifying Eq. (8), the following is obtained:

$$\boldsymbol{\Delta\omega} = \left\{ \begin{array}{c} \omega_r \\ 0 \\ \omega_h \end{array} \right\} - \left\{ \begin{array}{c} (\Delta\beta_0^2 - \Delta\beta_2^2)\omega_{\text{des}_r} - \Delta\beta_0\Delta\beta_2\omega_{\text{des}_h} \\ 0 \\ \Delta\beta_0\Delta\beta_2\omega_{\text{des}_r} + (\Delta\beta_0^2 - \Delta\beta_2^2)\omega_{\text{des}_h} \end{array} \right\} = \mathbf{0} \tag{31}$$

Since $\boldsymbol{\omega}_{\text{des}} = \boldsymbol{\omega}$, and $\Delta\beta_0^2 = 1 - \Delta\beta_2^2$, this yields the following system of equations in two variables:

$$\left[\begin{array}{cc} \omega_{\text{des}_r} & \omega_{\text{des}_h} \\ \omega_{\text{des}_h} & -\omega_{\text{des}_r} \end{array} \right] \left\{ \begin{array}{c} 2\Delta\beta_2^2 \\ 2\Delta\beta_1\Delta\beta_2 \end{array} \right\} = \mathbf{0}$$

For elliptic or hyperbolic orbits, $-\omega_{\text{des}_r}^2 - \omega_{\text{des}_h}^2 < 0$. Hence $\Delta\beta_2 = 0$, and consequently, $\Delta\beta_0 = 1$ as it has already been shown that $\Delta\beta_1$ and $\Delta\beta_3$ are zero. Therefore, it is clear that the set M contains only the origin. Hence any trajectory starting in Z, will asymptotically approach M, i.e, the origin as $t \to \infty$. The equilibrium is thus proven to be asymptotically stable and the controller drives the current trajectory to the desired trajectory asymptotically. Furthermore, since $V \to \infty$ as $|\mathbf{z}| \to \infty$, the

equilibrium is also globally stable.

It is interesting to note that $\omega_{\mathrm{des}_h} = 0$ for parabolic orbits, and $\dot{V}$ could be zero without $\Delta\beta_2$ and $\Delta\beta_0$ necessarily being zero (other error quantities are zero even in this case). As a consequence, the controller derived is not able to transfer from an elliptic orbit to a parabolic orbit, except for specific cases. An analogous conclusion is drawn in Ref. 2.

Appendix B: Closed-Loop Stability if Modeled Disturbances are Ignored

If the modeled disturbances are ignored in the control law, then the closed loop system has the following dynamics:

$$\Delta\ddot{r} + c_1\Delta\dot{r} + c_2\Delta r = d_r - d_{\mathrm{des}_r} \tag{32a}$$

$$\Delta'\dot{\omega}_h + c_3\Delta'\omega_h + c_4\Delta\beta_3 = \frac{d_\theta}{r} - \frac{d_{\mathrm{des}_\theta}}{r_{\mathrm{des}}} \tag{32b}$$

$$\Delta'\omega_r + c_5\Delta\beta_1 = \frac{d_h}{\omega_h r} - \frac{d_{\mathrm{des}_h}}{\omega_{\mathrm{des}_h} r_{\mathrm{des}}} \tag{32c}$$

It is known that in the absence of disturbances, the solutions to Eqs. (32) approach zero as $t \to \infty$. In the case where the modeled disturbance is the J_2 perturbation, the expressions on the right hand side are bounded by the maximum J_2 perturbation on the initial orbit and the minimum J_2 perturbation on the target orbit, or vice versa. In either case, from the Gronwall-Bellman Inequality,[24] the solutions to the above equations remain bounded within a region around zero; the limits of these bounds are proportional to J_2. To further simplify analysis, the radial error equation is considered, with the assumption that the errors in the EP equations are of the same order upon scaling by the radial distance. The "differential disturbance" acting on the system when the spacecraft is very close to its target orbit, is evaluated as $d_r - d_{\mathrm{des}_r} \approx \boldsymbol{\nabla} d_r^T\big|_{\mathrm{des}} (\mathbf{x} - \mathbf{x}_{\mathrm{des}})$, where d_r is given in Eq. (5), and $\mathbf{x}$ are the states in the closed-loop system. The evaluation of $\mathbf{x} - \mathbf{x}_{\mathrm{des}}$ requires the evaluation of the direct EP differences, denoted by $\boldsymbol{\Delta'\beta}$, which have the following relation with the

error EPs:

$$\boldsymbol{\Delta}'\boldsymbol{\beta} = \boldsymbol{\beta} - \boldsymbol{\beta}_{\text{des}} = \begin{bmatrix} \beta_{\text{des}_0} & -\beta_{\text{des}_1} & -\beta_{\text{des}_2} & -\beta_{\text{des}_3} \\ \beta_{\text{des}_1} & \beta_{\text{des}_0} & -\beta_{\text{des}_3} & \beta_{\text{des}_2} \\ \beta_{\text{des}_2} & \beta_{\text{des}_3} & \beta_{\text{des}_0} & -\beta_{\text{des}_1} \\ \beta_{\text{des}_3} & -\beta_{\text{des}_2} & \beta_{\text{des}_1} & \beta_{\text{des}_0} \end{bmatrix} \begin{Bmatrix} \Delta\beta_0 - 1 \\ \Delta\beta_1 \\ \Delta\beta_2 \\ \Delta\beta_3 \end{Bmatrix} \tag{33}$$

Using the above relation to compute the relative EPs from the differential EPs, a small change in the (i, j)th entry of the direction cosine matrix $\mathbf{C}$ is given by:

$$\Delta C_{13} = 2\left[C_{\text{des}_{13}}\left(\Delta\beta_0 - 1\right) - C_{\text{des}_{33}}\Delta\beta_2 + C_{\text{des}_{23}}\Delta\beta_3\right] \tag{34a}$$

$$\Delta C_{23} = 2\left[C_{\text{des}_{23}}\left(\Delta\beta_0 - 1\right) + C_{\text{des}_{33}}\Delta\beta_1 - C_{\text{des}_{13}}\Delta\beta_3\right] \tag{34b}$$

The radial equation reduces to:

$$\Delta\ddot{r} + c_1\Delta\dot{r} + c_2\Delta r = f_1\Delta r + f_2\Delta\beta_3 + f_3\Delta\beta_2 \tag{35}$$

where (setting $k = -3J_2\mu R_e^2/2$),

$$f_1 = -\frac{4k}{r_{\text{des}}^5}(1 - 3C_{\text{des}_{13}}^2), \quad f_2 = -\frac{12k}{r_{\text{des}}^4}C_{\text{des}_{13}}C_{\text{des}_{23}}, \quad f_3 = \frac{12k}{r_{\text{des}}^4}C_{\text{des}_{13}}C_{\text{des}_{33}}$$

Equations (32b) and (32c) can also be reduced likewise and the final result is a system of damped, multi-degree of freedom linear differential equations with periodic coefficients. The stability of this system can be analyzed using Floquet theory.[25] Consequently, though the controller stabilizes the system to a region around the equilibrium, the gains $c_{1\ldots5}$ have to take positive values, but cannot have arbitrarily small magnitudes. Ignoring cross coupling terms, the equation can be expressed as $\ddot{x} + c_1\dot{x} + c_2x = A\sin^2(nt)x$, where $A = 8k/a^5$. As an extreme case, a LEO reference is considered (where J_2 effects are maximum), so that $R_e/a \approx 1$. Choosing gains using the methodology outlined in the paper, $c_2 = n^2$ and $c_1 = 2n$. By changing the independent variable from t to $\tau = nt$, the equation reduces to $x'' + 2x' + x = 12J_2\sin^2\tau\ x$, which is the damped Mathieu equation. Analysis of this equation in Ref. 25 shows that it is asymptotically stable for this order of magnitude of damping

value and parametric excitation amplitude. Thus the control law is effective in orbital transfer even if J_2 terms are ignored.

References

[1] Ilgen, M. R., "Low Thrust OTV Guidance using Lyapunov Optimal Feedback Control Techniques," *Advances in the Astronautical Sciences*, Vol. 85(2), Univelt Inc., 1993, pp. 527–1545, AAS 93-680.

[2] Gurfil, P., "Control-Theoretic Analysis of Low-Thrust Orbital Transfer Using Orbital Elements," *Journal of Guidance, Control, and Dynamics*, Vol. 26, No. 6, November-December 2003, pp. 979–983.

[3] Chang, D. E., Chichka, D. F., and Marsden, J. E., "Lyapunov-based Transfer between Elliptic Keplerian Orbits," *Discrete and Continuous Dynamical Systems - Series 13*, Vol. 2, No. 1, February 2002, pp. 57–67.

[4] Schaub, H. and Alfriend, K. T., "Hybrid Cartesian and Orbit Element Feedback Law for Formation Flying Spacecraft," *Journal of Guidance, Control, and Dynamics*, Vol. 25, No. 2, March-April 2002, pp. 387–393.

[5] Schaub, H., Vadali, S. R., Junkins, J. L., and Alfriend, K. T., "Spacecraft Formation Flying Using Mean Orbital Elements," *The Journal of the Astronautical Sciences*, Vol. 48, No. 1, January-March 2000, pp. 69–87.

[6] Naasz, B. J., *Classical Element Feedback Control for Spacecraft Orbital Maneuvers*, Master's thesis, Virginia Polytechnic Institute and State University, Blacksburg, VA, May 2002.

[7] Wang, P. K. C. and Hadaegh, F. Y., "Minimum-Fuel Formation Reconfiguration of Multiple Free-Flying Spacecraft," *The Journal of the Astronautical Sciences*, Vol. 47, No. 1-2, January-June 1999, pp. 77–102.

[8] Junkins, J. L. and Turner, J. D., "On the Analogy Between Orbital Dynamics and Rigid Body Dynamics," *The Journal of the Astronautical Sciences*, Vol. 27, No. 4, October-December 1979, pp. 345–358.

[9] Kechichian, J. A., "Motion in General Elliptic Orbit with Respect to a Dragging and Precessing Coordinate Frame," *The Journal of the Astronautical Sciences*, Vol. 46, No. 1, January-March 1998, pp. 25–46.

[10] Carpenter, J. R., Leitner, J. A., Folta, D. C., and Burns, R. D., "Benchmark Problems for Spacecraft Formation Flight Missions," *AIAA Guidance, Navigation, and Control Conference and Exhibit*, No. AIAA-2003-5364, AIAA, Austin, TX, August 2003.

[11] Curtis, S. A., "The Magnetosphere Multiscale Mission... Resolving Fundamental Processes in Space Plasmas," Tech. Rep. NASA TM-2000-209883, NASA Science and Technology Definition Team for the MMS Mission, 1999.

[12] Clohessy, W. H. and Wiltshire, R. S., "Terminal Guidance System for Satellite Rendezvous," *Journal of Aerospace Sciences*, Vol. 27, September 1960, pp. 653–658, 674.

[13] Melton, R. G., "Time Explicit Representation of Relative Motion Between Elliptical Orbits," *Journal of Guidance, Control and Dynamics*, Vol. 23, No. 4, July-August 2000, pp. 604–610.

[14] Vaddi, S. S., Vadali, S. R., and Alfriend, K. T., "Formation Flying: Accommodating Nonlinearity and Eccentricity Perturbations," *Journal of Guidance, Control, and Dynamics*, Vol. 26, No. 2, March-April 2003, pp. 214–223.

[15] Schaub, H. and Alfriend, K. T., "J_2 Invariant Relative Orbits for Formation Flying," *International Journal of Celestial Mechanics and Dynamical Astronomy*, Vol. 79, 2001, pp. 77–95.

[16] Vadali, S. R., Vaddi, S. S., and Alfriend, K. T., "A New Concept for Controlling Formation Flying Satellite Constellations," *Advances in the Astronautical Sciences*, Vol. 108(2), Univelt Inc., 2001, pp. 1631–1648, AAS 01-218.

[17] Junkins, J. L. and Turner, J. D., *Optimal Spacecraft Rotational Maneuvers*, Elsevier, 1986.

[18] Vaddi, S. S., Alfriend, K. T., Vadali, S. R., and Sengupta, P., "Formation Establishment and Reconfiguration using Impulsive Control," *Journal of Guidance, Control, and Dynamics*, Vol. 28, No. 2, March-April 2005, pp. 262–268.

[19] Sengupta, P., Vadali, S. R., and Alfriend, K. T., "Modeling and Control of Satellite Formations in High Eccentricity Orbits," *The Journal of the Astronautical Sciences*, Vol. 52, No. 1-2, January-June 2004, pp. 149–168.

[20] Spencer, D. B. and Culp, R. D., "An Analytical Approach for Continuous-Thrust, LEO-GEO Transfers," *AIAA/AAS Astrodynamics Conference*, No. AIAA-1994-3760, AIAA, Scottsdale, AZ, August 1994, pp. 421–430.

[21] Grodzovskii, G. L., Ivanov, Y. N., and Tokayev, V. V., *Mechanics of Low-Thrust Spaceflight*, IPST Press, 1969.

[22] Battin, R. H., *An Introduction to the Mathematics and Methods of Astrodynamics*, AIAA Education Series, revised ed., 1999.

[23] Herman, A. L. and Spencer, D. B., "Optimal, Low-Thrust Earth-Orbit Transfers using Higher-Order Collocation Methods," *Journal of Guidance, Control, and Dynamics*, Vol. 25, No. 1, January-February 2002, pp. 40–47.

[24] Khalil, H. K., *Nonlinear Systems*, Prentice Hall, 3rd ed., 2002.

[25] José, J. V. and Saletan, E. J., *Classical Dynamics: A Contemporary Approach*, Cambridge University Press, 1998.

Figures

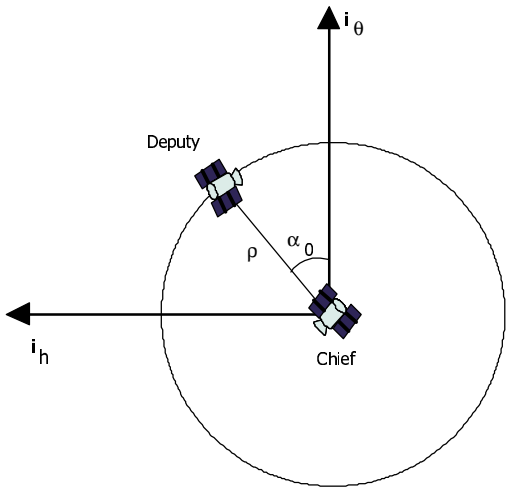

Figure 1 Relative Radius and Initial Phase Angle

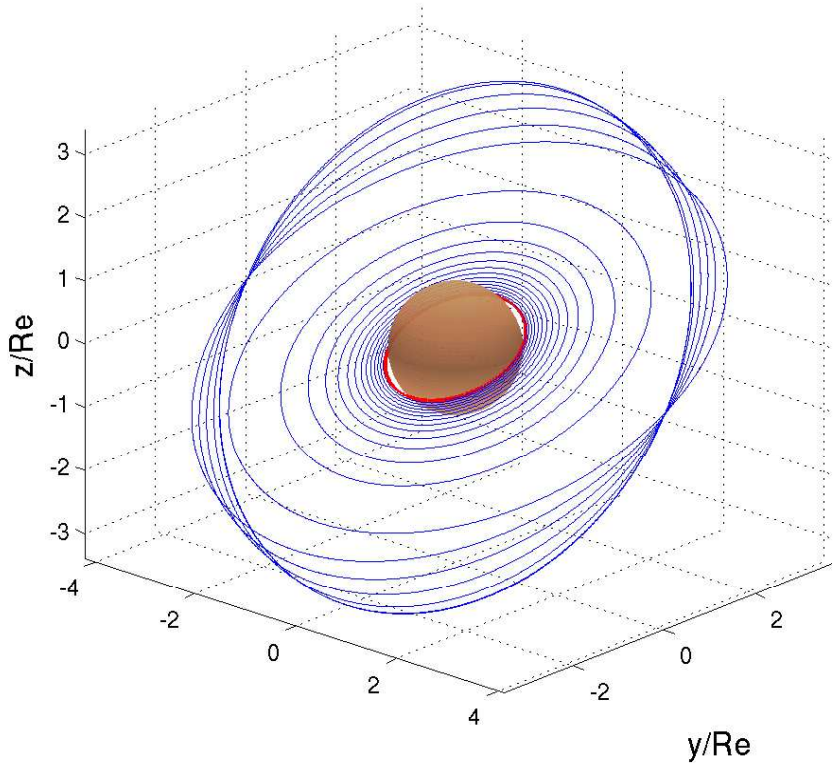

Figure 2 Orbital Transfer from LEO Parking to MEO Circular

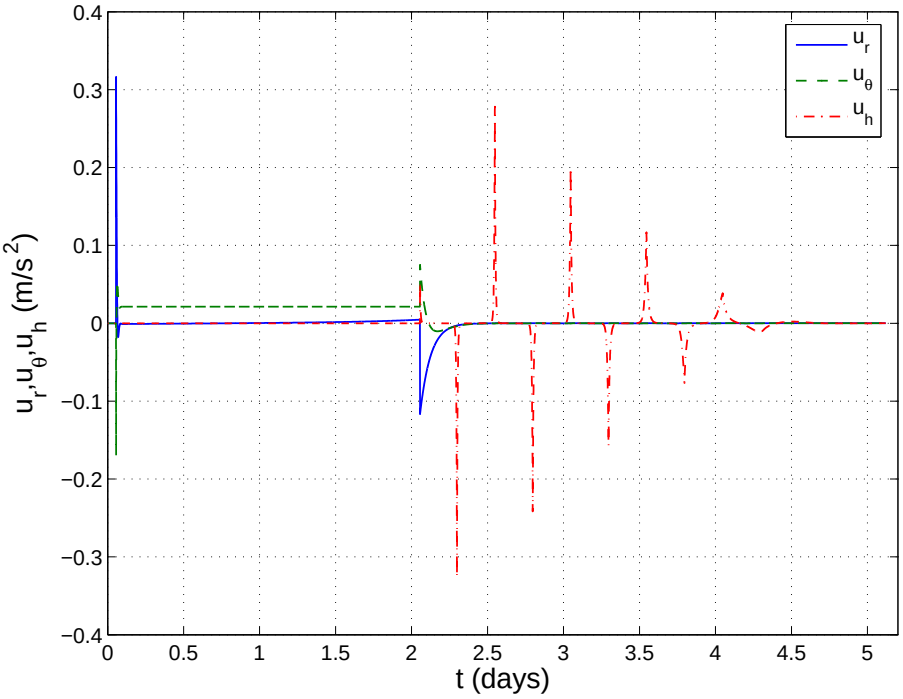

Figure 3 Control Profile for Orbital Transfer

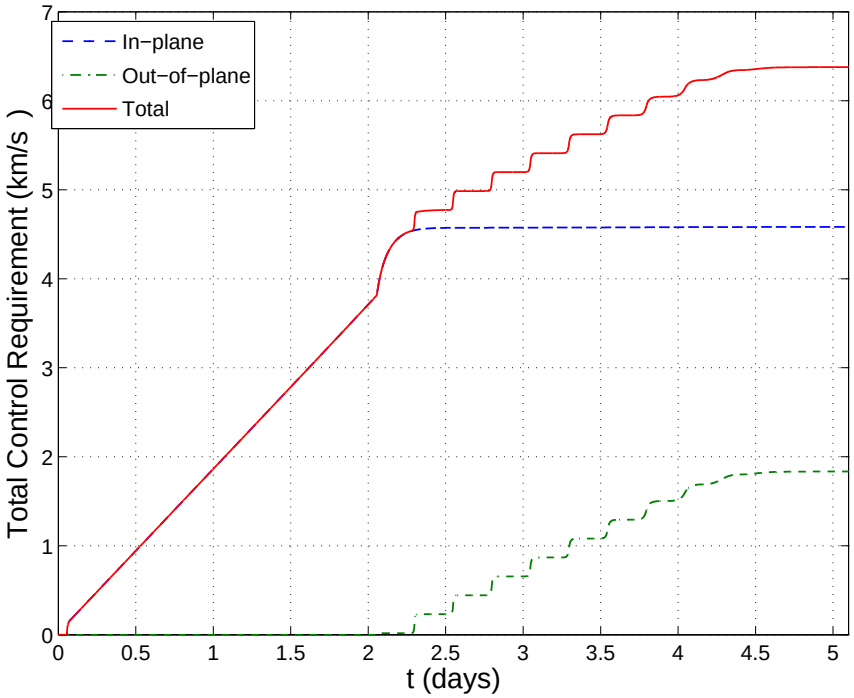

Figure 4 TCR for Orbital Transfer

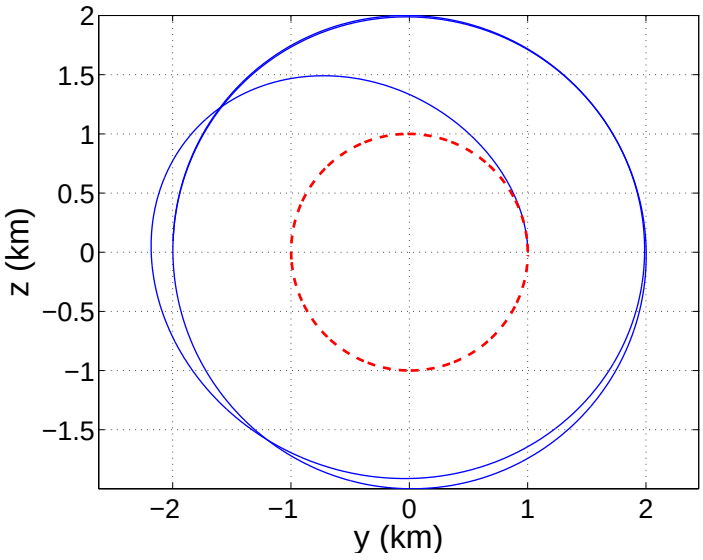

(i) Projection on θ-h plane

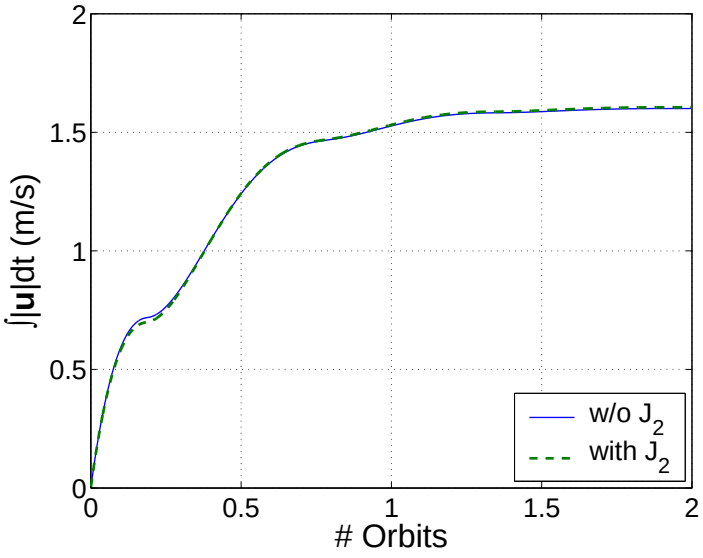

(ii) TCR

Figure 5 Lyapunov-based Reconfiguration Control: Projected Trajectory and TCR for Low-Eccentricity Reference, $\alpha_{0_i} = \alpha_{0_f} = 0^\circ$

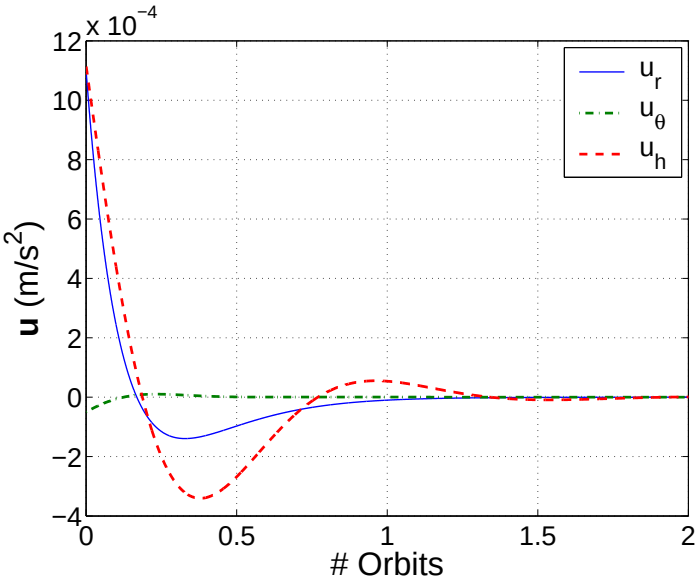

Figure 6 Lyapunov-based Reconfiguration Control: Control History for Low-Eccentricity Reference, $\alpha_{0_i} = \alpha_{0_f} = 0°$

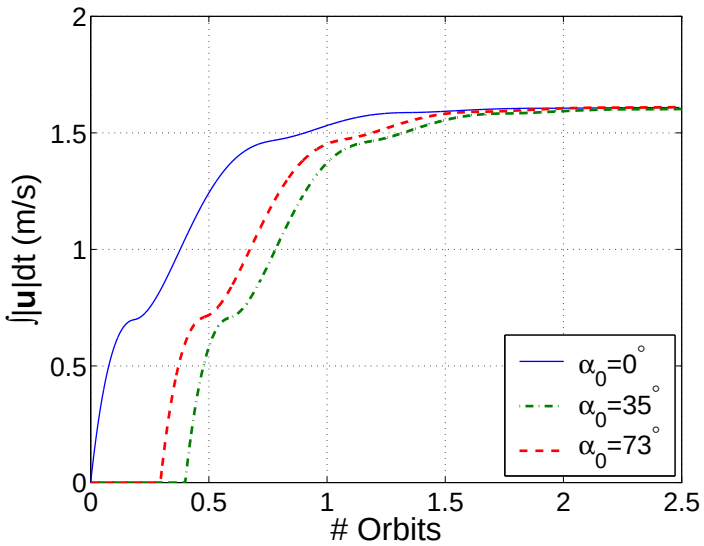

Figure 7 TCR for $\alpha_{0_i} = \alpha_{0_f} = \alpha_0$, Low-Eccentricity Reference

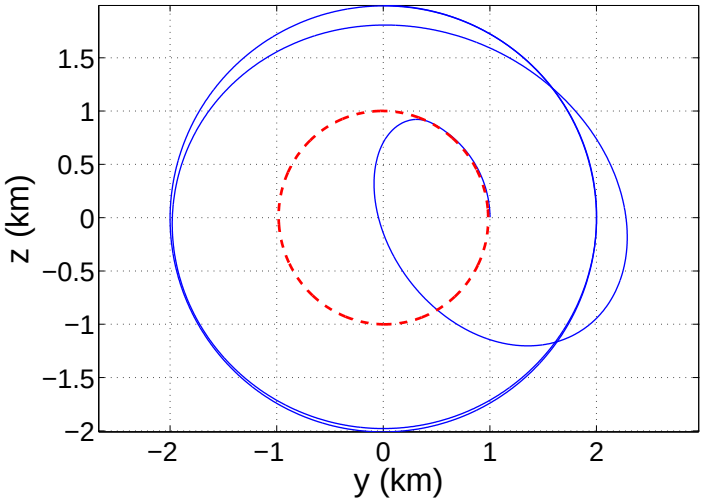

(i) Projection on θ-h plane

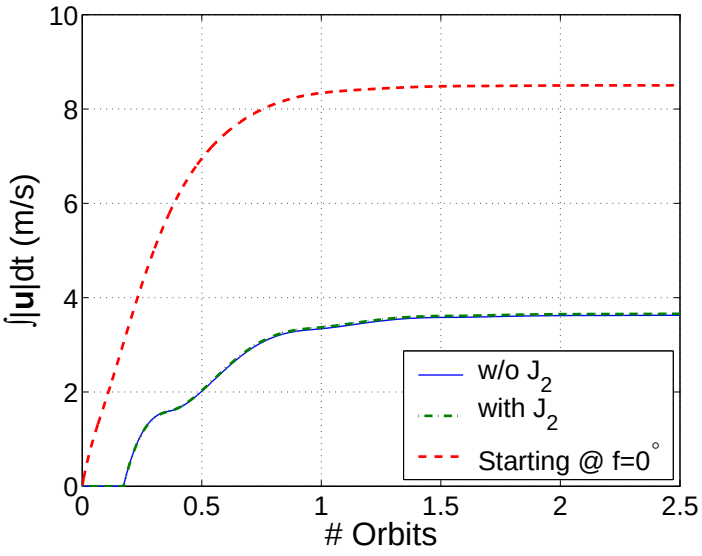

(ii) TCR

Figure 8 Lyapunov-based Reconfiguration Control: Projected Trajectory and TCR for Low-Eccentricity Reference, $\alpha_{0_i} = 0°$, $\alpha_{0_f} = 90°$

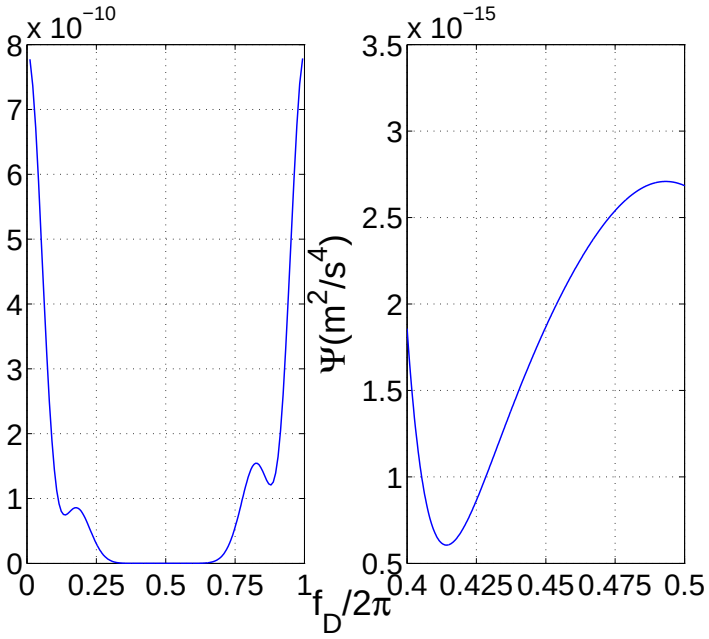

(i) Ψ

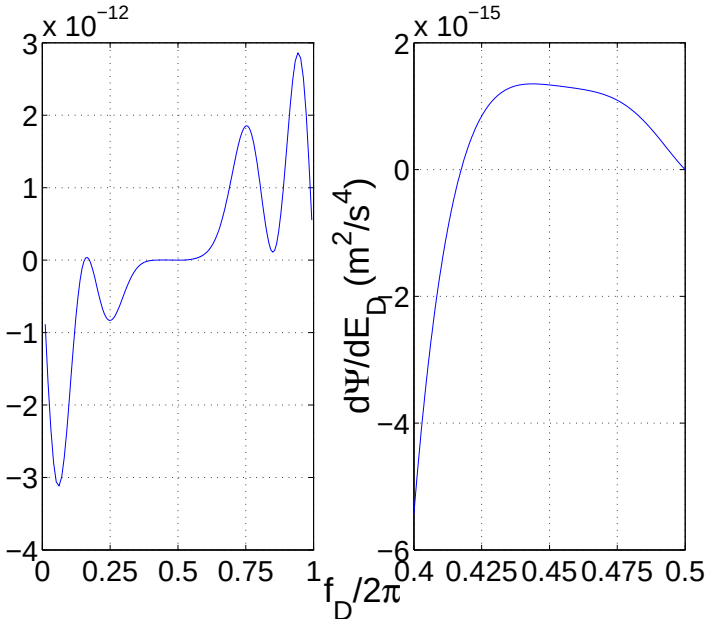

(ii) Ψ'

Figure 9 Variation of Ψ and $d\Psi/dE_D$, with True Anomaly, f_D, High Eccentricity Reference, $\alpha_{0_i} = \alpha_{0_f} = 0^\circ$

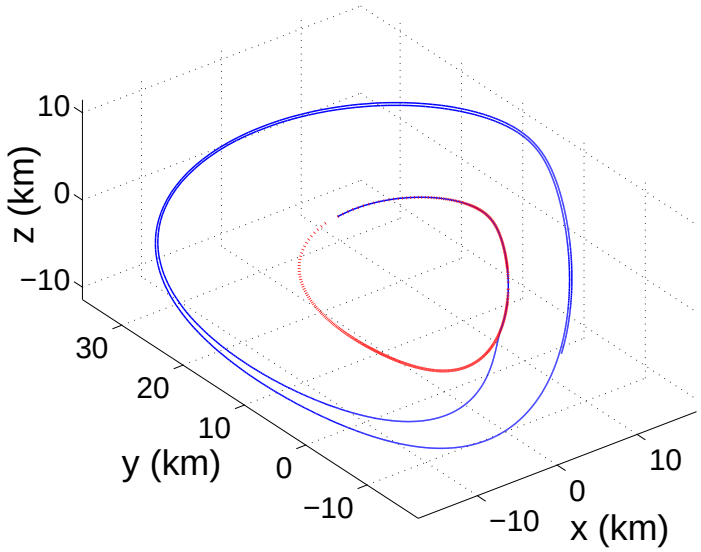

(i) Reconfiguration

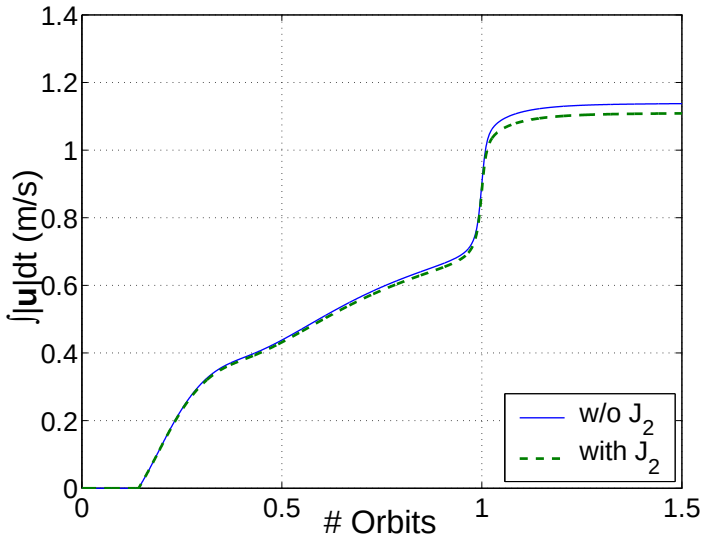

(ii) TCR

Figure 10 Lyapunov-based Reconfiguration Control: Trajectory and TCR for High-Eccentricity Reference, $\alpha_{0_i} = \alpha_{0_f} = 0^\circ$